

# Total reaction cross sections from elastic $\alpha$ -nucleus scattering angular distributions around the Coulomb barrier

P. Mohr,<sup>1,2,\*</sup> D. Galaviz,<sup>3</sup> Zs. Fülöp,<sup>2</sup> Gy. Gyürky,<sup>2</sup> G. G. Kiss,<sup>2,†</sup> and E. Somorjai<sup>2</sup>

<sup>1</sup> *Diakonie-Klinikum, D-74523 Schwäbisch Hall, Germany*

<sup>2</sup> *Institute of Nuclear Research (ATOMKI), H-4001 Debrecen, Hungary*

<sup>3</sup> *Centro de Fisica Nuclear, University of Lisbon, 1649-003 Lisbon, Portugal*

(Dated: November 17, 2018)

The total reaction cross section  $\sigma_{\text{reac}}$  is a valuable measure for the prediction of  $\alpha$ -induced reaction cross sections within the statistical model and for the comparison of scattering of tightly bound projectiles to weakly bound and exotic projectiles. Here we provide the total reaction cross sections  $\sigma_{\text{reac}}$  derived from our previously published angular distributions of  $\alpha$ -elastic scattering on  $^{89}\text{Y}$ ,  $^{92}\text{Mo}$ ,  $^{112,124}\text{Sn}$ , and  $^{144}\text{Sm}$  at energies around the Coulomb barrier.

PACS numbers: 24.10.Ht, 25.55.-e

The total reaction cross section  $\sigma_{\text{reac}}$  is related to the complex scattering matrix  $S_L = \eta_L \exp(2i\delta_L)$  by the well-known relation

$$\sigma_{\text{reac}} = \frac{\pi}{k^2} \sum_L (2L+1) (1 - \eta_L^2) \quad (1)$$

where  $k = \sqrt{2\mu E}/\hbar$  is the wave number, and  $\eta_L$  and  $\delta_L$  are the real reflexion coefficients and scattering phase shifts. Usually, experimental elastic scattering angular distributions are analyzed using a complex optical potential. Although there are considerable uncertainties in the extraction of the optical potential from elastic scattering at low energies around the Coulomb barrier, the underlying reflexion coefficients and phase shifts are well defined, as long as the measured angular distribution covers the full angular range from  $0^\circ$  to  $180^\circ$  and it is well described by the chosen optical potential. Thus, the total reaction cross section  $\sigma_{\text{reac}}$  can be extracted from experimental elastic scattering angular distributions with small uncertainties. Although the analysis uses optical potentials, i.e. input from theory, in practice the obtained total reaction cross section  $\sigma_{\text{reac}}$  can be considered an experimental quantity because of its insensitivity to the potential as long as the potential accurately reproduces the elastic scattering angular distribution.

A completely model-independent determination of  $\sigma_{\text{reac}}$  is also possible by a direct fit of the reflexion coefficients  $\eta_L$  and phase shifts  $\delta_L$  to the angular distribution. However, in practice such fits are not widely used because  $\eta_L$  and  $\delta_L$  have to be determined for angular momenta up to about  $L = 30$ , i.e. around 60 parameters have to be fitted simultaneously. This may lead to an oscillatory behavior of the calculated cross sections in angular regions where no experimental data are available to restrict the multi-parameter model-independent fit [1].

Therefore, model-independent analyses are not the ideal tool for the determination of total reaction cross sections  $\sigma_{\text{reac}}$ .

It has unfortunately become a common practice in optical model analyses of  $\alpha$ -elastic scattering data not to give  $\sigma_{\text{reac}}$  explicitly although this number is implicitly determined in any optical model calculation, as Eq. (1) shows. Nevertheless it has been noticed recently that  $\sigma_{\text{reac}}$  is a very valuable quantity in several respects. First, a significantly different energy dependence of  $\sigma_{\text{reac}}$  has been observed in the comparison of scattering of tightly bound projectiles like  $\alpha$  or  $^{16}\text{O}$ , weakly bound projectiles like  $^{6,7,8}\text{Li}$ , and exotic projectiles with halo properties like  $^6\text{He}$  and  $^{11}\text{Be}$  (e.g. [2–5]). As a consequence,  $\sigma_{\text{reac}}$  is practically always provided in analyses of  $^6\text{He}$  scattering. Second, the cross section of  $\alpha$ -induced reactions like e.g.  $(\alpha, \gamma)$ ,  $(\alpha, n)$ , or  $(\alpha, p)$  sensitively depends on the underlying  $\alpha$ -nucleus potential that is applied in statistical model calculations, e.g. for the prediction of reaction cross sections and stellar reaction rates for nuclear astrophysics [6–8]. In these calculations the total reaction cross section is taken as the formation cross section of the compound nucleus, and it is thus the basic building block for any prediction of reaction cross sections within the statistical model. (Note, however, that this basic prerequisite of the statistical model may be not fulfilled at very low energies where direct inelastic scattering may at least contribute to  $\sigma_{\text{reac}}$ .)

The present Brief Report provides the total reaction cross sections  $\sigma_{\text{reac}}$  from high precision  $\alpha$  scattering experiments performed at ATOMKI, Debrecen, Hungary [9–12]. These scattering data cover an angular range between  $20^\circ$  and  $170^\circ$  in steps of about  $1^\circ - 2^\circ$  and show small error bars below  $\approx 4\%$  over the whole angular range which is by far sufficient to derive the total reaction cross section with small uncertainties. These uncertainties in the determination of  $\sigma_{\text{reac}}$  from experimental elastic scattering angular distributions are briefly discussed.

Two experimental elastic scattering angular distributions of  $^{89}\text{Y}(\alpha, \alpha)^{89}\text{Y}$  at energies of  $E_{\text{c.m.}} = 15.51 \text{ MeV}$

\*Electronic address: WidmaierMohr@t-online.de

†present address: Laboratori Nazionali del Sud, INFN, Catania, Italia

and 18.63 MeV [9] are shown in Fig. 1 together with two different fits to the data at each energy. The first fit considers a folding potential in the real part and a combination of volume and surface Woods-Saxon potentials in the imaginary part of the nuclear optical potential; it is identical to the local potential in [9]. In the second fit the folding potential in the real part is replaced by a more flexible Woods-Saxon potential of volume type where all Woods-Saxon parameters have been readjusted. We find that both fits describe the data with similar  $\chi^2$  values. The resulting total reaction cross sections  $\sigma_{\text{reac}}$  at 15.51 MeV are 678 mb in the case of considering a folding potential and 683 mb for the Woods-Saxon potential and 1004 mb (folding) and 1009 mb (Woods-Saxon) at 18.63 MeV. The choice of the parameterization of the real nuclear potential (folding or Woods-Saxon) has a minor influence on the derived total reaction cross section of below 1%. Changes in the shape of the imaginary part also do not affect the extracted  $\sigma_{\text{reac}}$  significantly, as long as the experimental data are precisely described. Predictions from global optical potentials typically agree with the  $\sigma_{\text{reac}}$  obtained from experiments within 5% in the  $^{89}\text{Y}$  case (for further details of global potentials for the  $^{89}\text{Y}-\alpha$  system, see discussion in [9]).

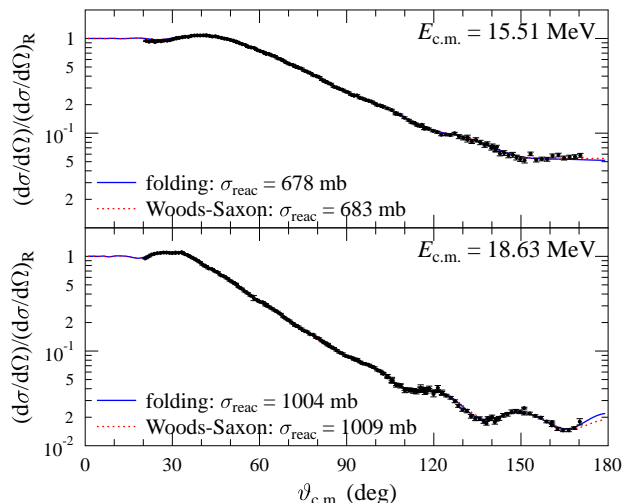


FIG. 1: (Color online) Rutherford normalized elastic scattering cross sections of the  $^{89}\text{Y}(\alpha, \alpha)^{89}\text{Y}$  reaction at  $E_{\text{c.m.}} = 15.51$  MeV and 18.63 MeV versus the angle in center-of-mass frame. The lines are calculated from a folding potential (full blue line) and from a Woods-Saxon potential (dotted red line) in the real part of the nuclear optical potential, and a combined volume and surface Woods-Saxon potential in the imaginary part. Both calculations accurately reproduce the angular distributions and thus provide almost the same total reaction cross section  $\sigma_{\text{reac}}$ .

Because of the minor influence of the chosen potential parameterization we list the total reaction cross sections  $\sigma_{\text{reac}}$  of  $^{89}\text{Y}$  [9],  $^{92}\text{Mo}$  [10],  $^{112,124}\text{Sn}$  [11], and  $^{144}\text{Sm}$  [12] from the original folding potential analyses of the given papers. The results are summarized in Table I.

TABLE I: Total reaction cross sections  $\sigma_{\text{reac}}$  derived from the  $\alpha$ -elastic angular distributions of  $^{89}\text{Y}$  [9],  $^{92}\text{Mo}$  [10],  $^{112,124}\text{Sn}$  [11], and  $^{144}\text{Sm}$  [12].

target	$E_{\text{c.m.}}$ (MeV)	$\sigma_{\text{reac}}$ (mb)
$^{89}\text{Y}$	15.51	$678 \pm 20$
$^{89}\text{Y}$	18.63	$1004 \pm 30$
$^{92}\text{Mo}$	13.20	$238 \pm 7$
$^{92}\text{Mo}$	15.69	$578 \pm 17$
$^{92}\text{Mo}$	18.62	$883 \pm 26$
$^{112}\text{Sn}$	13.90	$93 \pm 3$
$^{112}\text{Sn}$	18.84	$695 \pm 21$
$^{124}\text{Sn}$	18.90	$760 \pm 23$
$^{144}\text{Sm}$	19.45	$404 \pm 12$

The absolute normalization of the experimental angular distributions is an important prerequisite for the accurate determination of the total cross section  $\sigma_{\text{reac}}$ . Fortunately, it can be taken from data at very forward angles where the scattering cross section is given by the Rutherford cross section. The smallest measured angle has to reach the range where the angular distribution does not deviate from the Rutherford cross section by more than 1%. The huge Rutherford cross sections at forward angles typically lead to high count rates, and thus a careful deatime correction is required. Furthermore, the steep angular dependence of the Rutherford cross section requires a precise angular calibration. These requirements are fulfilled by our experiments, and the resulting uncertainty in the absolute normalization of our experimental data is of the order of 1%; for details, see Refs. [9–12].

The data at backward angles strongly affect the imaginary part of the potential which in turn determines the deviations of the reflexion coefficients  $\eta_L$  from unity. (Obviously,  $\eta_L = 1$  for all angular momenta  $L$  and thus  $\sigma_{\text{reac}} = 0$  is found for all nuclear potentials without imaginary part.) Typical uncertainties of individual data points at backward angles remain below 3–4% (mainly defined by statistics). Together with the huge number of data points in [9–12] the shape of the angular distribution is well-defined within 2% over the full measured angular range. In a simple view, the total reaction cross section  $\sigma_{\text{reac}}$  is approximately given by the deviation of the measured angular distribution from the Rutherford cross section, and the uncertainty of the backward angular distribution enters directly into the uncertainty of  $\sigma_{\text{reac}}$ .

Combining the above uncertainties of less than 1% from the choice of the potential, about 1% from the absolute normalization at forward angles, about 2% from the backward cross sections, and 1% from the not measured angular range above  $170^\circ$ , this leads to a total uncertainty of about 3% for  $\sigma_{\text{reac}}$  from the analysis of the scattering data of [9–12] using error quadratic summing.

Finally, in Fig. 2 we compare the new total reaction cross sections of  $\alpha$ -induced reactions to a series of data for exotic nuclei ( $^6\text{He}$ ), weakly bound nuclei ( $^{6,7,8}\text{Li}$ ), and

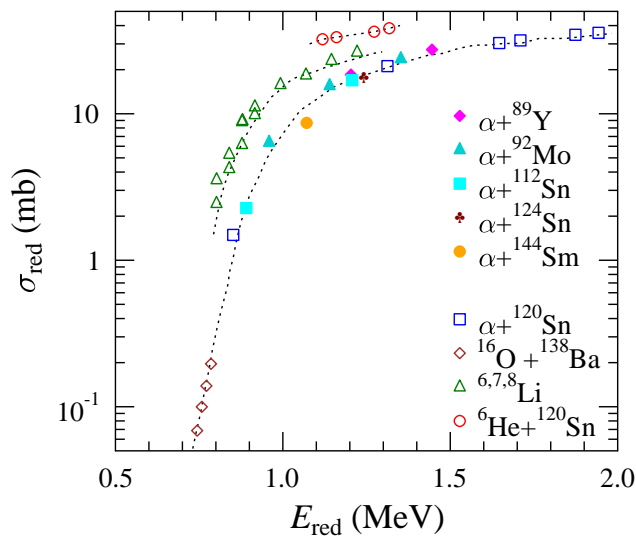


FIG. 2: (Color online) Reduced reaction cross sections  $\sigma_{\text{red}}$  versus reduced energy  $E_{\text{red}}$  for tightly bound  $\alpha$ -particles and  $^{16}\text{O}$ , weakly bound  $^{6,7,8}\text{Li}$  projectiles, and exotic  $^6\text{He}$ . (Update of Fig. 4 from [3] with additional data from [13]). The error bars of the new data (full data points) are omitted because they are smaller than the point size. The lines are to guide the eye.

tightly bound particles ( $\alpha$  or  $^{16}\text{O}$ ); this is basically an update of Fig. 4 of [3] with new additional data points from this study and from  $^{120}\text{Sn}$  [13]. For this comparison we use the so-called reduced energy  $E_{\text{red}}$  and reduced reaction cross section  $\sigma_{\text{red}}$  which are given by

$$E_{\text{red}} = \frac{(A_P^{1/3} + A_T^{1/3})E_{\text{c.m.}}}{Z_P Z_T} \quad (2)$$

$$\sigma_{\text{red}} = \frac{\sigma_{\text{reac}}}{(A_P^{1/3} + A_T^{1/3})^2} \quad (3)$$

The reduced energy  $E_{\text{red}}$  takes into account the different heights of the Coulomb barrier in the systems under consideration, whereas the reduced reaction cross section  $\sigma_{\text{red}}$  scales the measured total reaction cross section  $\sigma_{\text{reac}}$  according to the geometrical size of the projectile-plus-target system. A smooth behavior for all  $\sigma_{\text{red}}$  of  $\alpha$ -induced reactions is found. The obtained values for  $\sigma_{\text{red}}$  are smaller for tightly bound projectiles ( $\alpha$ ,  $^{16}\text{O}$ ) compared to weakly bound projectiles ( $^{6,7,8}\text{Li}$ ) and halo projectiles ( $^6\text{He}$ ). The lines in Fig. 2 are shown to guide the eye (taken from [3]). A deeper theoretical understanding of these different energy dependencies will be helpful for the prediction of reaction cross sections within the statistical model.

In conclusion, we have extracted total reaction cross sections  $\sigma_{\text{reac}}$  from our previously published experimental  $\alpha$  scattering data on  $^{89}\text{Y}$ ,  $^{92}\text{Mo}$ ,  $^{112,124}\text{Sn}$ , and  $^{144}\text{Sm}$  [9–12]. The derived cross sections  $\sigma_{\text{reac}}$  have small uncertainties of about 3% and show a smooth and systematic energy dependence which is consistent with other  $\alpha$ -scattering results and data for another tightly bound projectile  $^{16}\text{O}$ . The energy dependence of the derived reduced cross section  $\sigma_{\text{red}}$  significantly differs from reactions induced by weakly bound and exotic projectiles with halo properties like e.g.  $^6\text{He}$ .

## Acknowledgments

We thank R. Lichtenthaler for encouraging discussions and providing the data of their Fig. 4 of Ref. [3]. This work is part of the EUROGENESIS project and was supported by OTKA (K68801, NN83261) and European Research Council grant agreement no. 203175.

- 
- [1] O. S. van Roosmalen, Phys. Rev. C **35**, 977 (1987).  
[2] A. Di Pietro, G. Randisi, V. Scuderi, L. Acosta, F. Amorini, M. J. G. Borge, P. Figuera, M. Fisichella, L. M. Fraile, J. G3mez-Camacho, H. Jeppesen, M. Lattuada, I. Martel, M. Milin, A. Musumarra, M. Papa, M. G. Pellegriti, F. Perez-Bernal, R. Raabe, F. Rizzo, D. Santonocito, G. Scalia, O. Tengblad, D. Torresi, A. Maira Vidal, D. Voulot, F. Wenander, M. Zadro, Phys. Rev. Lett. **105**, 022701 (2010).  
[3] P. N. de Faria, R. Lichtenthaler, K. C. C. Pires, A. M. Moro, A. L3p3ne-Szily, V. Guimar3es, D. R. Mendes, A. Arazi, M. Rodr3guez-Gallardo, A. Barioni, V. Morcelle, M. C. Morais, O. Camargo, J. Alcantara Nu3ez, M. Assun33o, Phys. Rev. C **81**, 044605 (2010).  
[4] N. Keeley, N. Alamanos, K. W. Kemper, K. Rusek, Prog. Part. Nucl. Phys. **63**, 396 (2009).  
[5] G. R. Satchler, Phys. Rep. **199**, 147 (1991).  
[6] M. Avrigeanu, W. von Oertzen, A. Obreja, F. L. Roman, V. Avrigeanu, At. Data Nucl. Data Tables **95**, 501 (2009).  
[7] T. Rauscher, Nucl. Phys. **A725**, 295 (2003).  
[8] P. Demetriou, C. Grama, S. Goriely, Nucl. Phys. **A707**, 253 (2002).  
[9] G. G. Kiss, P. Mohr, Zs. F3l3p, D. Galaviz, Gy. Gy3rky, Z. Elekes, E. Somorjai, A. Kretschmer, K. Sonnabend, A. Zilges, M. Avrigeanu, Phys. Rev. C **80**, 045807 (2009).  
[10] Zs. F3l3p, Gy. Gy3rky, Z. M3t3, E. Somorjai, L. Zolnai, D. Galaviz, M. Babilon, P. Mohr, A. Zilges, T. Rauscher, H. Oberhammer, G. Staudt, Phys. Rev. C **64**, 065805 (2001).  
[11] D. Galaviz, Zs. F3l3p, Gy. Gy3rky, Z. M3t3, P. Mohr, T. Rauscher, E. Somorjai, and A. Zilges, Phys. Rev. C **71**, 065802 (2005).  
[12] P. Mohr, T. Rauscher, H. Oberhammer, Z. M3t3, Zs. F3l3p, E. Somorjai, M. Jaeger, G. Staudt, Phys. Rev. C **55**, 1523 (1997).  
[13] P. Mohr, P. N. de Faria, R. Lichtenthaler, K. C. C. Pires, V. Guimar3es, A. L3p3ne-Szily, D. R. Mendes Junior, A.

Arazi, A. Barioni, V. Morcelle, M. C. Morais, Phys. Rev. C , submitted.